APPLICATION OF A MAXIMUM LIKELIHOOD TYPE ESTIMATOR TO THE TOWED ARRAY SHAPE ESTIMATION PROBLEM

Robert Been

TNO Physics and Electronics Laboratory, Underwater Acoustics Group, Observation Systems Dept.; P.O. Box 96864, 2509 JG The Hague, The Netherlands; telephone: +31 70 374 0475, fax: +31 70 328 0961, e-mail: Been@fel.tno.nl, URL: http://www.tno.nl/instit/fel

1 INTRODUCTION

At the TNO Physics and Electronics Laboratory (TNO-FEL), for a number of decades, the behaviour and performance of towed sonar systems has been studied extensively. Since the performance of towed sonars highly depends on the shape of the hydrophone array, the underwater acoustics group started performing research in this field in the 1980's. Currently, the study of array shape and the processing aspects of non-linear arrays is an important part of the TNO-FEL Low Frequency Active Sonar (LFAS) programme. Part of the work in this field is performed in collaboration with Thomson Sintra Activités Sous-Marines (TS.ASM) in a project referred to as Shape Corrected Beamforming (SCB).
Some research topics considered in these projects are:

- the identification of losses that result from acoustic aperture deformation;
- the development of towed array shape estimators based on non-acoustic sensor output, such estimators are to operate in real-time;
- the validation of towed array shape estimators by means of simulated data;
- the validation of towed array shape estimators by means of sea-trial data, using the TNO-FEL shot-firing method [1];
- signal processing aspects of time-varying, curved arrays.

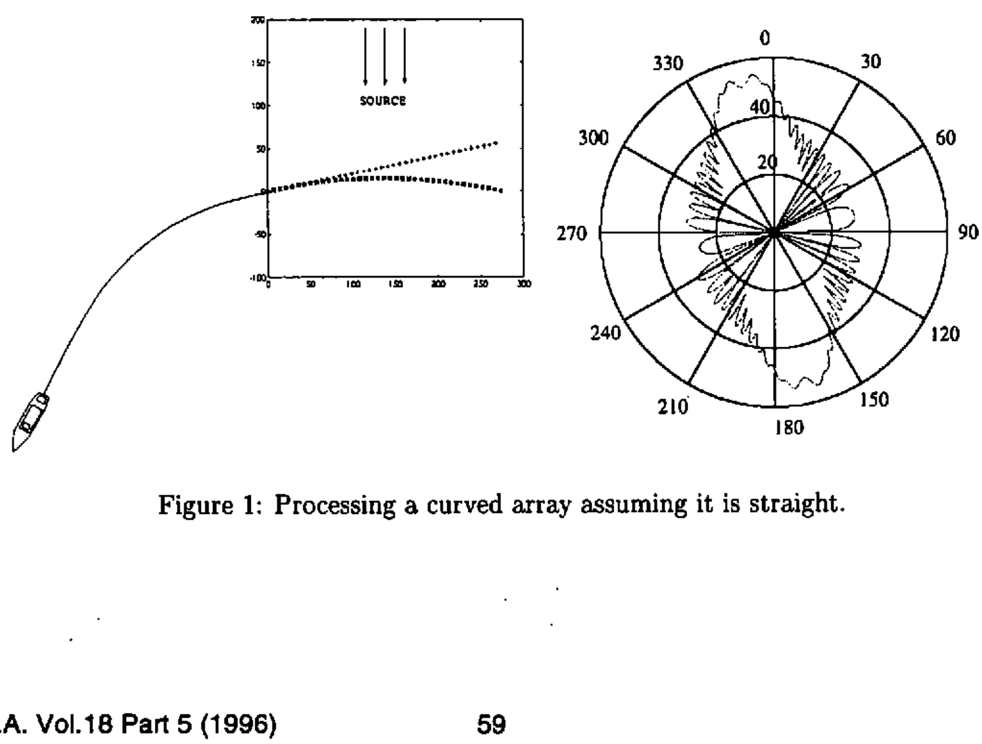

Figure 1: Processing a curved array assuming it is straight.

APPLICATION OF A ML TYPE ESTIMATOR TO THE TA SHAPE ESTIMATION PROBLEM

Figures 1 and 2 illustrate the main consequences of processing a curved array under the assumption that it is straight: gain loss, main lobe widening, an angular error and sidelobe rising.

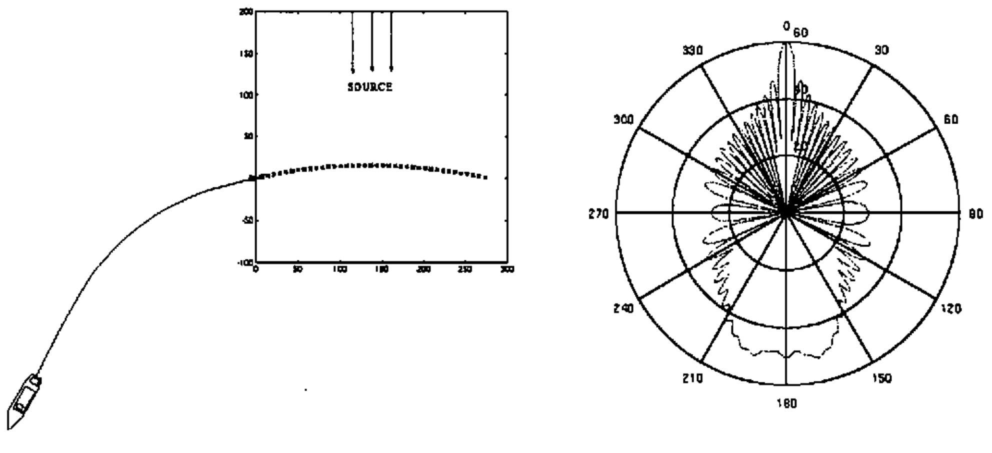

Figure 2: Processing a (static) curved towed array taking into account the acoustic aperture shape.

There are several ways, known from literature, to correct for the array deformation and consequently repair the losses described above. Two possible approaches to solve the specified problem are:

1. acoustic beamformer output optimisation; optimisation of the beamformer output as a function of array shape using an underlying hydrophone array model, mostly by making use of a target of opportunity (e.g. [2]);

2. towed array shape estimation using non-acoustic sensor data, such as heading and depth data, and an underlying hydrodynamic hydrophone array model; this method is used in combination with a dynamic beamformer, see e.g. [3, 4, 5].

we have opted for methods that use data from in-hose sensors rather than acoustic methods that mostly require a target of opportunity. This paper describes an algorithm that estimates the 3-D towed array shape evolving in time, from both heading and depth sensor data. The motivation for the choice of this specific algorithm is given in Section 2, the algorithm description is given in Section 3.

Of course, these towed array shape estimators will have to be validated. This is done by using both simulated and sea-trial data. The advantage of using simulated data is that one is able to work with well-defined and cheap experiments. Sea-trial data will have to be used because of the fact that even the best model will not be able to approach reality well enough. In other words, sea-trial data will be used to observe estimator performance under operational conditions.
The simulated reference data, that consists of 3-D cable and array positions as well as artificial heading and depth data, have been generated by using a full-scale hydrodynamic sonar system model developed at TNO-FEL. This model is based on [6]. An example is given in Section 4.
The alternative method used to generate reference hydrophone array shape data, this time using sea-trial measurements, is the shot-firing method. This method generates snapshots of the acoustic aperture by means of explosive charges, with a maximum rate of three per minute. The shot-firing method, as opposed to fixed test ranges, can perform under normal working conditions at any location, provided there is sufficient bottom depth; for more details see [1]. The heading and depth data that are used to reconstruct the array shape (prior to beamforming the acoustic hydrophone data), has been recorded during these shot-firing experiments. Shot-firing data has been recently collected by using the TNO-FEL LFAS system. The validation methods

described above are depicted in Figure 3.

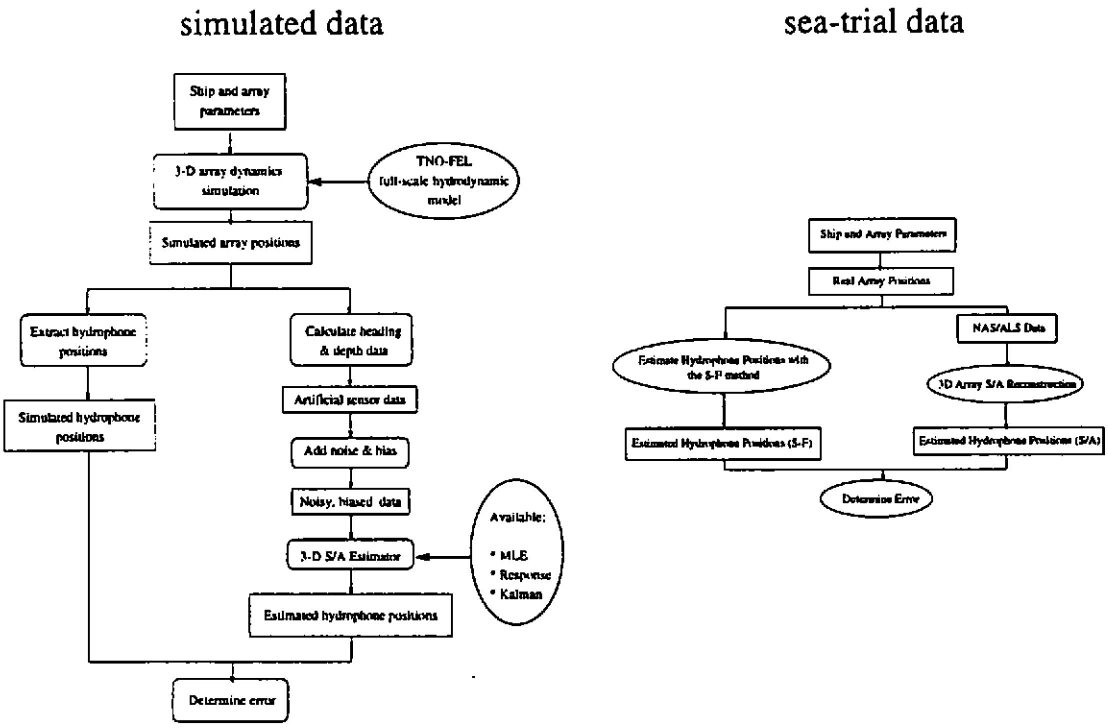

Figure 3: Research outline for the validation of a towed array shape estimator.

The reconstruction of the array shape alone is not sufficient to repair the losses that result from processing a curved array. The next step is designing a beamformer capable of processing an array with a time-varying (estimated) geometry, see Section 5. From literature, a number of candidate algorithms are known, cf. [4, 5, 7]. The TNO-FEL SCB programme aims at designing practicable, validated, real-time dynamic beamforming concepts, that enable towing vessels to continue using their towed sonar effectively during turns. One of the results of this programme will be a demonstrator, that is to be installed on board HNLMS Tydeman, which is kindly provided by the Royal Netherlands Navy (RNLN) for performing sea-trials with the TNO-FEL LFAS system. See Figure 4 for a graphical representation of the demonstrator.

2 DESCRIPTION AND LIMITATIONS OF THE CHOSEN APPROACH

Our approach to designing a towed array shape estimator that may be used during towing vessel manoeuvres, starts from the method as described in Gray [3]. This article presents an elegant way to solve the towed array shape estimation problem, using an underlying hydrodynamic model to describe the hydrophone array motion in combination with a Kalman filter. However, the hydrodynamic model-based estimator given in [3], has been designed for small perturbations around a rectilinear towed array shape. Especially the hydrodynamic model description of the array is based on this assumption.
The equation on which all approximations are based, is Païdoussis' equation, cf. [8, 9]:

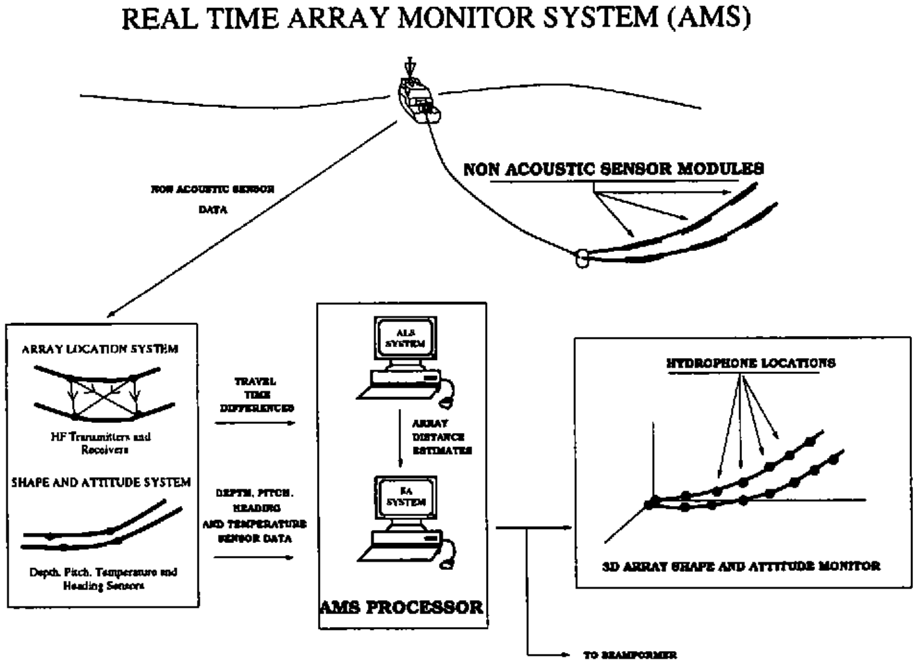

Figure 4: Graphical representation of the TNO-FEL SCB demonstrator.

$$EI\frac{\partial^4 y}{\partial x^4} + F_T\frac{\partial y}{\partial x} - \frac{\partial}{\partial x}\left(\left(\frac{1}{2}c_t\frac{L_a - x}{d_a} + \frac{1}{2}c_2\right)MU^2\frac{\partial y}{\partial x}\right)$$
$$+M\left(\frac{\partial}{\partial t} + U\frac{\partial}{\partial x}\right)^2 y + \frac{1}{2\pi}c_n\frac{MU}{d_a}\left(\frac{\partial y}{\partial t} + U\frac{\partial y}{\partial x}\right) + m\frac{\partial^2 y}{\partial t^2} = 0, \quad (1)$$

where:

$y(x,t)$	displacement of the array	[m];
x	space variable increasing downstream	[m];
t	time	[s];
EI	the flexural rigidity or bending stiffness	[kg m^3 s^{-2}];
m	the mass per unit length	[kg m^{-1}];
M	the virtual mass per unit length of the fluid	[kg m^{-1}];
d_a	the diameter of the array	[m];
U	the tow speed along the x-axis	[m s^{-1}];
L_a	the array length	[m];
F_T	the viscous forces per unit length in the tangential direction	[kg m^{-1}];
c_t	the tangential drag coefficient of the cylinder	[-];
c_n	the normal drag coefficient of the cylinder	[-];
c_2	the coefficient of form drag of the trailing end	[-].

In this equation the orientation of the x-axis has been chosen parallel to the flow velocity. The tow point is always situated on the y-axis, see Figure 5. Again, please note that the equation and the observed coordinate system have been constructed to describe the perturbed array shape around a nominally straight line.

APPLICATION OF A ML TYPE ESTIMATOR TO THE TA SHAPE ESTIMATION PROBLEM

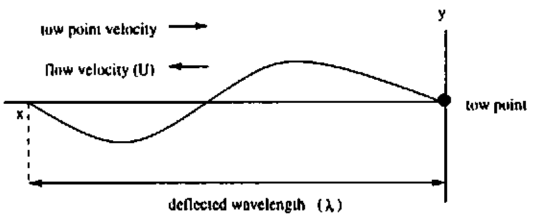

Figure 5: Birds-eye view on the array coordinate system.

The 3-D array shape 'reality' has been reduced to two separate 2-D models (x, y plane and the s, z plane), as proposed by Païdoussis, Ketchman [10] and Kennedy. Moreover, Equation 1 has been simplified by Kennedy and Gray. The various simplifications to Païdoussis' original array model are depicted in Figure 6.

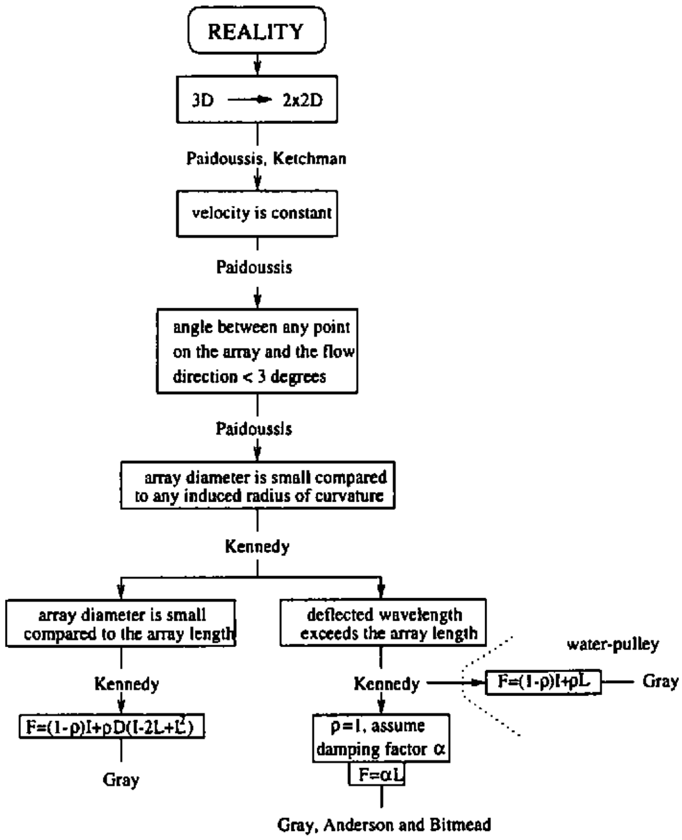

Figure 6: Simplifications to Païdoussis' original hydrophone array model.

The worm-in-a-hole (or water-pulley) model, has been used in [3] and [11]. We used it as a starting point for the description of array behaviour during turns:

$$\tilde{\rho}\frac{\partial \eta}{\partial s} + \frac{\partial \eta}{\partial t} = 0, \tag{2}$$

APPLICATION OF A ML TYPE ESTIMATOR TO THE TA SHAPE ESTIMATION PROBLEM

where $\tilde{\rho} = \frac{\pi c_t + c_n}{c_n}$, and where η may denote both slope a and depth d. s denotes the arc length along the array.
This model, that we applied in our estimator, basically assumes that each point of the array follows the track of the tow point; it can be readily applied as a starting point for modelling hydrophone array behaviour during a towing vessel manoeuvre. We used it with this difference, however, that we applied a Maximum Likelihood type estimator, cf. [12]. The advantage of the state-space description we adapted from Gray is that we can still use the estimator should we need a more sophisticated hydrodynamic array model. This might be the case when designing an optimum ML type estimator that is to be used during towing vessel turns.
Moreover, multiple array configurations can also be addressed using this estimator, even if this should introduce non-linearities into the system description. For the Target Motion Analysis (TMA) problem, which in a way resembles the problem presented in this paper, the ML estimator has proven to be capable of dealing with such system non-linearities, again see [12].
A description of the ML type estimator applied to the towed array shape estimation problem is given in the next section.

3 TOWED ARRAY SHAPE ESTIMATION ALGORITHM DESCRIPTION

The ML type estimator, like the Kalman filter, uses a state-space representation for the towed array system: a state equation to describe the towed array motion evaluating in time, and a measurement equation that connects the measured quantities to the elements of the state vector.

3.1 State equation

The worm-in-a-hole model serves as a basis for our state equation. Like Païdoussis and Ketchman [10] proposed, the 3-D array shape model has been decoupled into two submodels which describe the state evolution in the x, y plane (bird's eye view), and the state evolution in the s, z plane (side view).
The state equation is obtained by discretisation of Equation 2 for both the array segment slope and depth. The chosen state vector $\mathbf{x}_k$ has the form:

$$\mathbf{x}_k = \begin{bmatrix} a_1 \\ a_2 \\ \vdots \\ a_{N-1} \\ d_1 \\ d_2 \\ \vdots \\ d_N \end{bmatrix}, \tag{3}$$

where k denotes time $t = k\Delta t$ with Δt the system temporal sample interval, a_i denotes the segment slope at the ith node of the discretised array, and d_i the depth at the ith nodal position. N is the number of array nodes. The slope is defined by the sine of the array segment heading, cf. Figure 7. Using the worm-in-a-hole model, the state equation is given by, cf. [3]:

$$\mathbf{x}_{k+1} = F\mathbf{x}_k + \mathbf{u}_k, \tag{4}$$

where:

$$F = \begin{bmatrix} (1-\rho)\, I^{(N-1)\times(N-1)} + \rho L & 0 \\ 0 & (1-\rho)\, I^{N\times N} + \rho L \end{bmatrix}, \tag{5}$$

APPLICATION OF A ML TYPE ESTIMATOR TO THE TA SHAPE ESTIMATION PROBLEM

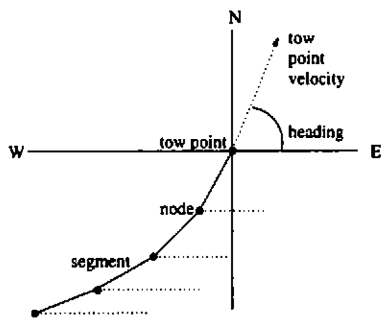

Figure 7: Definition of the coordinate system.

where I is the identity matrix, $L = \begin{bmatrix} 0 & 0 & . & . & 0 \\ 1 & 0 & . & . & . \\ 0 & 1 & 0 & . & . \\ . & . & . & . & . \\ 0 & . & . & 1 & 0 \end{bmatrix}$, and $\rho = \bar{\rho}\frac{\text{temporal discretisation interval}}{\text{spatial discretisation interval}}$.

$\mathbf{u}_k$ is the steering vector, which in this application contains both the slope of the first array node and the depth of the first node:

$$\mathbf{u}_k = \rho \begin{bmatrix} a_1^k \\ 0 \\ \vdots \\ 0 \\ d_1^k \\ 0 \\ \vdots \\ 0 \end{bmatrix} \quad \begin{matrix} \\ 1 \\ \vdots \\ N-2 \\ \\ 1 \\ \vdots \\ N-1 \end{matrix} \tag{6}$$

In towed array practice, however, the steering vector is (partly) unknown. We can use the output of the first heading and depth sensor for this purpose, the only disadvantage is that these measured quantities are corrupted by noise and possibly even bias, cf. [13]. Since the sensor outputs are the only information we have, the only thing we can hope for is that $\mathrm{E}(\tilde{a}_1^k) = a_1^k$ and $\mathrm{E}\left(\tilde{d}_1^k\right) = d_1^k$. Of course, the slope and depth data may also be pre-processed.

Another problem for using this state equation in towed array practice, is that it starts from a constant towing speed. In practice, this is rarely the case. Our approach to overcome this problem, is to construct a piecewise constant approximation of the speed, and 'skip' from one state equation to another whenever the assumed speed changes.

3.2 Measurement equation

Since the measured quantities are themselves elements of the state vector, the measurement equation is linear and very simple in its form:

$$\mathbf{y}_k = C\mathbf{x}_k + \omega_k, \tag{7}$$

$\mathbf{y}_k \in \mathrm{IR}^{2M\times 1}$, where M is the number of heading/depth sensor packages. C is:

$$C = \begin{bmatrix} H_a & 0 \\ 0 & H_d \end{bmatrix}, \tag{8}$$

APPLICATION OF A ML TYPE ESTIMATOR TO THE TA SHAPE ESTIMATION PROBLEM

where $H_a(j,n) = \delta_{p_j n}$, for $j = 1,\ldots,M$, and $n = 1,\ldots,N-1$, thereby assuming M heading/depth sensor packages at positions $p_1, p_2, \ldots, p_M$ along the array; hence: $H_d(j,n) = \delta_{p_j n}$, for $j = 1,\ldots,M$, and $n = 1,\ldots,N$. ω_k denotes the measurement noise, which is assumed to be zero-mean Gaussian white noise: $N\left(0,\sigma_a^2\right)$ for the slope and $N\left(0,\sigma_d^2\right)$ for the depth.
Furthermore, bias may be present, which is likely to be the case when in-hose sensors are used. The flexible hose-wall might cause mounting dispositions, which vary slowly in time. In [13], this problem is discussed. We will not address this topic in this paper, however.
Note that for a multiple array system, where inter-array distances are added to the measurement equation, Equation 8 will become non-linear.

3.3 The state estimator

The ML type estimator is a batch-type estimator. The way in which we use it here is as an estimator that calculates the state vector $\mathbf{x}_k$ from a set of measurements $Z_W = \{\mathbf{y}_{k-W+1},\ldots,\mathbf{y}_k\}$, where W denotes the size of the measurement data set, i.e. the number of sensor station samples that are used.
The maximum likelihood estimate $\hat{\mathbf{x}}_k$ of the state vector $\mathbf{x}_k$ is the mode of the conditional probability density function

$$p\left(Z_W \mid \mathbf{x}\right) = \frac{1}{(2\pi)^{MW}\sigma_a^{MW}\sigma_d^{MW}} \exp\left(-\frac{1}{2}\sum_{i=k-W+1}^{i=k} \mathbf{r}_i^T\mathbf{r}_i\right), \tag{9}$$

where the weighted residuals $\mathbf{r}_i$ are defined by:

$$\mathbf{r}_i = \begin{bmatrix} \frac{I^{M\times M}}{\sigma_a} & \\ & \frac{I^{M\times M}}{\sigma_d} \end{bmatrix} \left(\mathbf{y}_i - C\mathbf{x}_i\right); \tag{10}$$

and where $\mathbf{x}$ denotes $\left[\mathbf{x}_{k-W+1}\ldots\mathbf{x}_k\right]^T$.
By using the negative log-likelihood function $L\left(Z_W,\mathbf{x}\right)$, the estimation problem is reduced to a non-linear least squares problem:

$$\hat{\mathbf{x}}_k = \min_{\mathbf{x}} L\left(Z_W,\mathbf{x}\right) \tag{11}$$

We used a Newton-type minimisation method to generate the state vector estimate:

1. Find a feasible starting point;
2. Stop if the optimality and convergence conditions are satisfied, i.e. the ML estimate must satisfy $\nabla_{\mathbf{x}} L\left(Z_W,\hat{\mathbf{x}}_k\right) = J^T\mathbf{r} = 0$;
3. Find a direction of search such that:
   $L\left(Z_W,\mathbf{x}^n + \alpha^n\mathbf{q}^n\right) < L\left(Z_W,\mathbf{x}^n\right)$,
   from:
   $H\mathbf{q}^n = -\mathbf{g}$, with $H = J^TJ + Q$, $\mathbf{g} = J^T\mathbf{r}$, $J^T = \nabla_{\mathbf{x}}\mathbf{r}^T$, and $Q = \sum_{i=k-W+1}^{k}\mathbf{r}_i\nabla_{\mathbf{x}}^2\mathbf{r}_i$.
   $\mathbf{r} = \left[\mathbf{r}_{k-W+1}\ldots\mathbf{r}_k\right]^T$, the operator $\nabla_{\mathbf{x}}$, finally, is defined by: $\nabla_{\mathbf{x}} = \left[\frac{\partial}{\partial\mathbf{x}_{k-W+1}}\cdots\frac{\partial}{\partial\mathbf{x}_k}\right]^T$;
4. $\mathbf{x}^{n+1} = \mathbf{x}^n + \alpha^n\mathbf{q}^n$, where α^n corresponds to the line minimum of the cost function along the direction $\mathbf{q}^n$;
5. goto step 2.

APPLICATION OF A ML TYPE ESTIMATOR TO THE TA SHAPE ESTIMATION PROBLEM

4 EXAMPLE

For illustration we discuss the results for a simulated 90 degree turn. We simulated both the 3-D array positions and the non-acoustic sensor data by using our full-scale hydrodynamic model based on [6]. The scenario observed here is defined by:

- the tow ship performs a 90 degree port turn;
- the tow ship speed is 8 kts throughout the manoeuvre;
- the radius of the turn is ≈230 m;
- array design frequency is 250 Hz;
- the hydrophone spacing $\Delta = 0.5\lambda$;
- $\sigma_s = 0.3$ deg, $\sigma_d = 0.3$ m;
- Δt=2 seconds;
- W=50;
- configuration:
  - cable: 1000 m;
  - hydrophone array: 765 m.

Table 1: Parameters for the towed array configuration.

	length [m]	diameter [m]	weight in air [kg/m^3]	c_t	c_n
cable	1000	0.027	2500.0	0.009	1.50
array	765	0.085	1027.0	0.004	1.50

The output of the ML type estimator has been compared with both the Kalman filter and the 'Response' results, of which the latter has already been validated with sea-trial data [11]. For this example, the results appeared to be comparable; the ML estimator even performs somewhat better than the other two estimators.

Some notes on the results which are presented in Figures 9 through 10:

- we used the quartic spline technique, [14], to interpolate from nodal to hydrophone positions;
- the beam patterns that are shown are based on the classical delay and sum principle;
- the figures show the estimated beam pattern evolving in time, based on the reconstructed array shape and attitude; in the figures, a line connects the beam pattern maxima;
- note that the gain loss is relative to the gain obtained with the *simulated*, hence the best possible reconstructed, array shape and attitude, *not* a straight array;
- the beam width used here is the 3 dB beam width;
- note that for interpretational purposes, both the reconstructed and simulated array data have been rotated towards the positive x-axis (over the same angle) before the beam pattern calculation, cf. Figure 8;

- for the beam pattern calculation, the broadside case has been considered, since it has the smallest beam width in general.

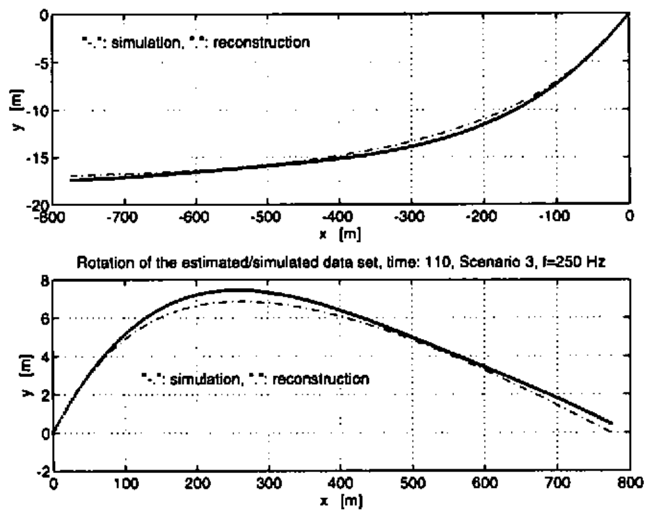

Figure 8: Rotation of both the simulated and reconstructed data set towards the positive x-axis.

5 PRELIMINARY VIEW ON THE DYNAMIC BEAMFORMER

Solving the towed array shape and attitude estimation problem is not sufficient to enable a towing vessel equipped with a towed sonar to continue processing during a turn. The acoustic hydrophone data will have to be processed taking the (estimated) time-varying towed array shape into account.
There are several dynamic beamformers known from literature, varying from relatively simple to sophisticated, e.g. [4, 5, 7].

Here, we restrict ourselves to a very simple narrow-band frequency-domain delay and sum beamformer. This might not be such a disadvantage, since classical beamforming is known to be very robust; i.e. the beamformer output is not extremely sensitive to hydrophone estimation errors, which is the case for most adaptive beamformers.

The approach we have followed for a possible real-time application, is to subdivide the array up into a number of straight sub-arrays. Consequently, these sub-arrays are processed, corrected for their relative inter-segment angles and summed accordingly. The number of segments required are determined as follows, note that this strategy could also be applied for determining the number of state vector elements. Consider the array placed on a circle that corresponds to the narrowest manoeuvre that is to be carried out by the towing vessel, say 300 metres. The number of segments could be chosen in such a way that the maximum path-length difference of any point on the array segment to its original position on the array does not exceed $\frac{1}{10}\lambda$. For the example as shown in the previous section, applying this criterion results in dividing the array into 20 segments, cf. Figure 12. Note that the strategy proposed here, resembles the approach followed by [7]. The method used by Fuchs, however, is more advanced since he takes account of the local curvature of the array.
The dynamic beamformer approach followed here turns out to be very time-efficient, since the array shape estimation process supplies us with the segment slopes. Consequently, the array is assumed to be piecewise

APPLICATION OF A ML TYPE ESTIMATOR TO THE TA SHAPE ESTIMATION PROBLEM

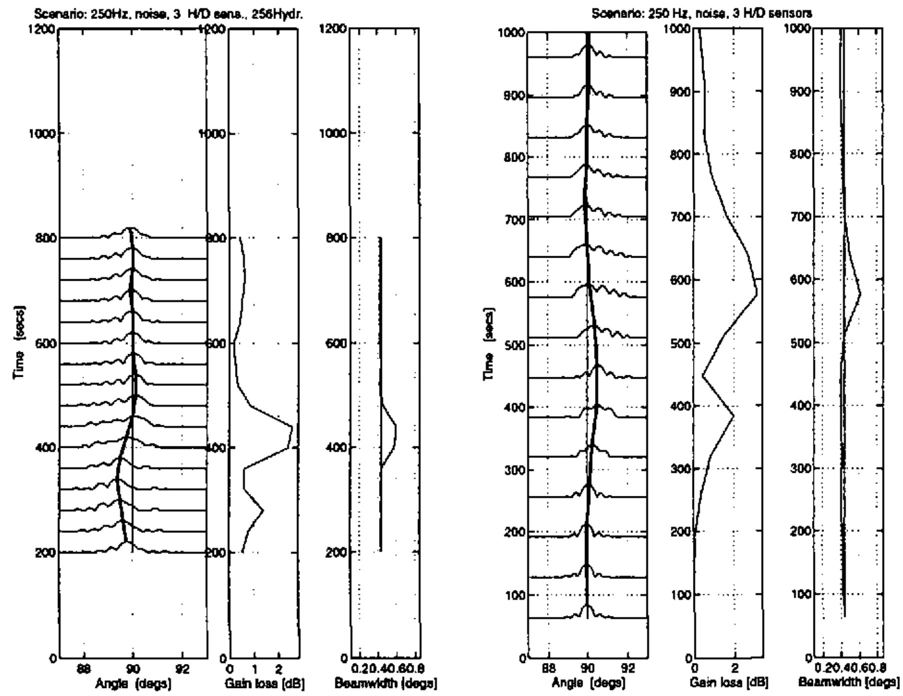

Figure 9: Results after applying the TNO-FEL 'Response' model (l) and results after applying the one-step Kalman predictor (r).

APPLICATION OF A ML TYPE ESTIMATOR TO THE TA SHAPE ESTIMATION PROBLEM

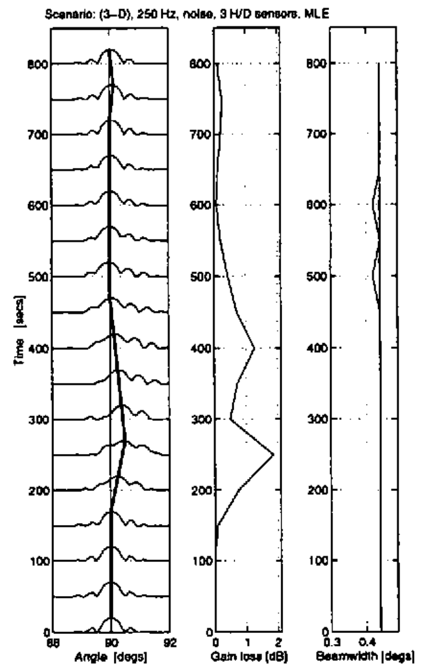

Figure 10: Results after applying the ML type estimator.

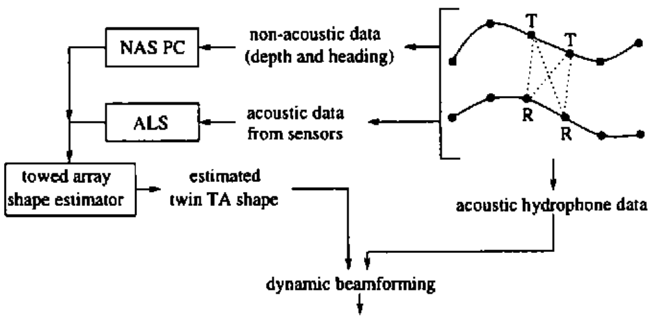

Figure 11: Beamformer

APPLICATION OF A ML TYPE ESTIMATOR TO THE TA SHAPE ESTIMATION PROBLEM

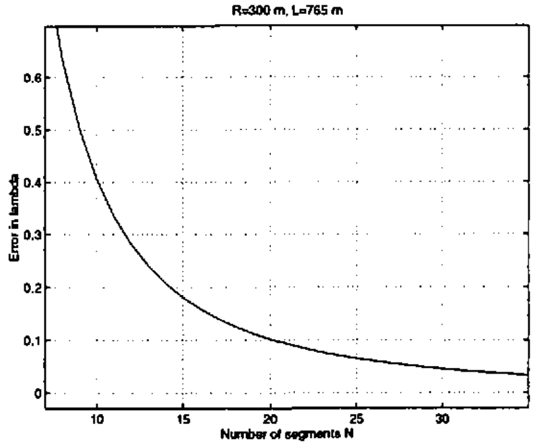

Figure 12: Maximum hydrophone position error as a function of the number of segments.

linear and is processed using FFT methods. The array shape update rate could be chosen to be equal to the time step Δt chosen earlier on.
An example result is now given with the array shape from the previous section at $t = 250$ seconds. We have processed the real (simulated) array shape, the estimated array shape and the piecewise-linear approximation of the estimated array shape. Figure 13 depicts the result of processing these arrays, with a target azimuth angle of 90 degrees.

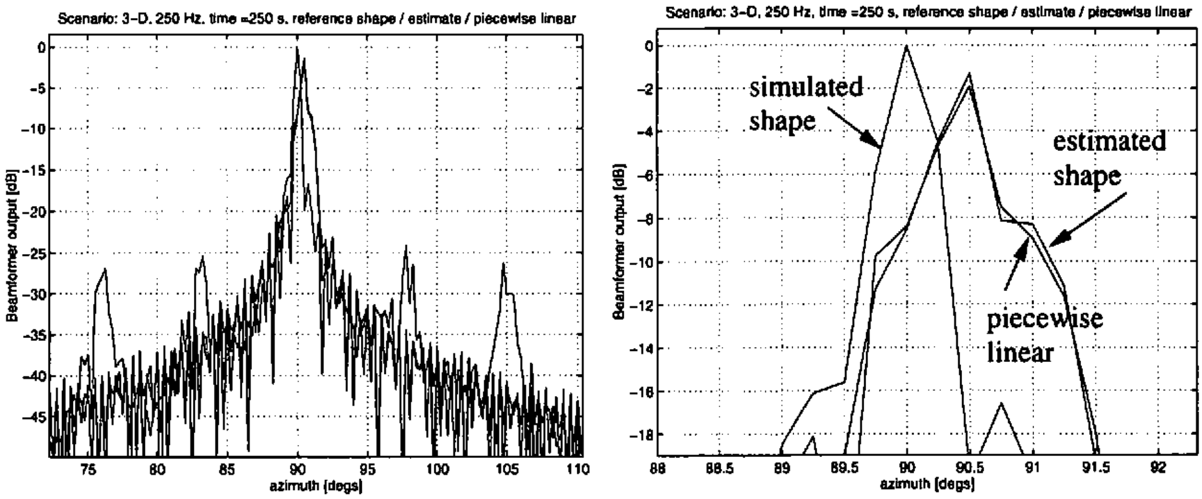

Figure 13: Processing results for the various array shapes.

6 CONCLUSIONS

In this paper we described the development of a ML type estimator that is to be used for towed array shape estimation during turns.
The estimator is based on a very simple hydrodynamic hydrophone array model, in combination with a cost

function minimisation technique that is capable of dealing with system non-linearities. Hence, the estimator may be used for multiple array towed sonars.
An example that reflects the quality of the estimator relative to other estimators, has been given. The results appeared to be comparable. We expect to obtain better results if we are able to fit a more sophisticated hydrodynamic array model into the system state-space description.
In future, we will also look for an optimum array shape estimator beamformer combination, that can be applied in the TNO LFAS system.

7 ACKNOWLEDGEMENTS

The author would like to thank the Royal Netherlands Navy for their support to the TNO-FEL array shape estimation and shape corrected beamformer programme. The author would also like to thank TS.ASM for their support.

REFERENCES

[1] E.C. van Ballegooijen et al., "Measurement of towed array position, shape and attitude", *IEEE Journ. Ocean. Eng.*, vol. 14, no. 4, Oct. 1989.

[2] B.G. Ferguson, "Sharpness applied to the adaptive beamforming of acoustic data from a towed array of unknown shape", *J. Acoust. Soc. Am.*, vol. 88, no. 6, pp. 2695–2701, 1990.

[3] D.A. Gray, B.D.O. Anderson, and R.R. Bitmead, "Towed array shape estimation using Kalman filters - theoretical models", *IEEE Journal of Oceanic Engineering*, 1993.

[4] H. Fan and X. Hu, "Tracking of conventional beamforming with hydrophone array of varying geometry", IEEE Transactions on Aerospace and Electronic Systems, vol. 28, no. 2, April 1992.

[5] W.S. Hodgkiss and V.C. Anderson, "Hardware dynamic beamforming", *J. Acoust. Soc. Am.*, vol. 69, no. 4, pp. 1075–1083, April 1981.

[6] F. Milinazzo, M. Wilkie, and S.A. Latchman, "An efficient algorithm for simulating the dynamics of towed cable systems", *Ocean Engng*, vol. 14, no. 6, pp. 513–526, 1987.

[7] J.J. Fuchs, "Shape calibration for a nominally linear equispaced array", *IEEE Transactions on Signal Processing*, 1995.

[8] M.P. Païdoussis, "Stability of towed, totally submerged flexible cylinders", *J. Fluid Mech.*, vol. 34, no. 2, pp. 273–297, 1968.

[9] M.P. Païdoussis, "Dynamics of cylindrical structures subjected to axial flow", *Journal of Sound and Vibration*, 1973.

[10] J. Ketchman, "Vibration induced in towed linear underwater array cables", *IEEE Journal of Oceanic Engineering*, 1981.

[11] C.S.van Aartsen, "The Response model - an operational model for towed array shape and attitude estimation from measurements by heading and depth sensors, validated on trial data.", in *Electronics Division Colloquium on "Heading Sensors for Sonar and Marine Applications*, 1994.

[12] J.H. de Vlieger and R.H.J. Gmelig Meyling, "Maximum likelihood estimation for long-range target tracking using passive sonar measurements", *IEEE Transactions on Signal Processing*, 1992.

[13] D.A. Gray, J.L. Riley, and D.H. Holdsworth, "Effect of biased compasses on towed array shape estimates obtained from Kalman filters", in *Acoustic Signal Processing for Ocean Exploration*, 1993, pp. 231–236.

[14] B.E. Howard and J.M. Syck, "Calculation of the shape of a towed underwater acoustic array", *J. Oceanic Engineering*, vol. 17, no. 2, pp. 193–203, April 1992.